

Розглянуто можливість створення аеромагнітної системи відведення об'єктів космічного сміття з низьких навколосезних орбіт. Особливістю конструкції даної аеромагнітної системи відведення є застосування магнітних органів керування відносним положенням аеродинамічного елемента з використанням постійних поворотних магнітів, що екрануються за допомогою спеціальних капсул екранів зі створами. Слід зазначити, що ця система пропонується для аеродинамічно нестійких космічних апаратів. Також, для аналізу працездатності і переваг застосування аеромагнітної системи відведення з постійними магнітами було запропоновано відповідний дискретний закон керування магнітними органами. Керування відносним положенням аеродинамічного елемента в орбітальній системі координат здійснюється з метою орієнтації і стабілізації його перпендикулярно до динамічного потоку атмосфери, що набігає. Проведене математичне моделювання орбітального руху космічного апарату під час відведення за допомогою аеромагнітної системи з постійними магнітами з різних орбіт. Було визначено, що при здійсненні стабілізації аеродинамічного елемента перпендикулярно до вектору динамічного потоку атмосфери, що набігає, час відведення зменшується на 25 % у порівнянні з неорієнтованим пасивним відведенням. Однак ця перевага у часі відведення властива лише для аеродинамічних елементів, площа Міделя яких значно більша за четверту частину площі повної поверхні. Так, слід зазначити, що проектування аеромагнітних систем відведення доцільно лише із використанням аеродинамічних вітрильних елементів, що розгортаються, і зовсім не є ефективним для великих надувних елементів.

Таким чином, розробка аеромагнітної системи відведення об'єктів космічного сміття з органами керування на постійних магнітах розширює межі ефективного застосування аеродинамічних вітрильних систем. В свою чергу, застосування магнітних органів з постійними магнітами дає новий напрямок для подальших досліджень керування орієнтацією великогабаритних космічних систем при мінімальних витратах палива та бортової енергії

Ключові слова: аеромагнітна система відведення, постійні магніти, космічний апарат, дискретний закон керування

UDC 629.78
DOI: 10.15587/1729-4061.2019.179382

DEVELOPMENT OF THE AEROMAGNETIC SPACE DEBRIS DEORBETING SYSTEM

E. Lapkhanov

Postgraduate student*

E-mail: Ernando@i.ua,

ericksaavedralim@gmail.com

S. Khoroshylov

Doctor of Technical Sciences, Senior

Researcher, Leading Researcher*

E-mail: skh@ukr.net

*Department of System Analysis

and Control Problems

Institute of Technical Mechanics of the

National Academy of Sciences of Ukraine

and the State Space Agency of Ukraine

(ITM of NASU and SSAU)

Leshko-Popelya str., 15, Dnipro,

Ukraine, 49005

Received date 09.08.2019

Accepted date 25.09.2019

Published date 28.10.2019

Copyright © 2019, E. Lapkhanov, S. Khoroshylov

This is an open access article under the CC BY license

(<http://creativecommons.org/licenses/by/4.0>)

1. Introduction

More space debris (SD) in Earth's orbits creates obstacles to the proper functioning of space technology units. Thus, according to [1], approximately 14,495 space debris objects (SDOs) were catalogued in Earth's orbits by the National Aeronautics and Space Administration (NASA) as of 1 April 2019.

The main sources of SDOs are the upper stages of launch vehicles, spacecraft (SC) at the end of active life, and fragments of SDOs of various origins. In turn, the most clogged areas of outer space were found to be low Earth orbits (LEOs) with altitudes ranging from 400 km to 2,000 km as well as geosynchronous high elliptical orbits [2, 3].

The problems of space clearance are solved with the help of active and passive means of removing SDOs [4–8]. Active SDO deorbiting means include collector spacecraft (CSC) with contact or contactless effect on SDOs, as well as electromagnetic devices and propulsion systems. Electromagnetic devices and motor units mounted on space-

craft to generate the braking impulse after the active life is completed are considered in [6–8]. Passive SDO removal means include systems that operate without requiring any control of the SC's assigned deorbiting motion. Such systems include aerodynamic deorbiting systems (ADDSSs), electrodynamic tethers (EDTs), electromagnetic deorbiting systems (EMDSSs), and permanent magnet deorbiting systems (PMDSSs) [4, 5].

It should be noted that the aforementioned passive SDO deorbiting systems do not require fuel consumption and have virtually no onboard energy requirements for their operation (except for EMDSSs). Each of the active or passive SDO removal systems has its advantages and disadvantages, with recommendations for use in different space missions for the clearance of Earth's orbital space from SD [9]. Based on analysing the specificity of missions for the clearance of Earth's space from SD [9], the need is also substantiated for further development of a promising direction to create hybrid deorbiting systems (HDSs). The main purpose of this area is to expand the boundaries of effective use of existing

SD disposal facilities. Thus, the present study proposes to extend the boundaries of the effective use of expandable, aerodynamic deorbiting sail systems by equipping them with permanent magnet devices. Such modernization of sailing ADDSs will reduce the time of SD removal from the LEOs, with minimal onboard energy consumption, which is quite relevant for orbits with significant levels of clogging. Moreover, the development of low-cost deorbiting systems for the orientation of large-scale space systems to which the ADDSs relate is a promising direction in the development of large orbital industrial and energy modules.

2. Literature review and problem statement

The current state of developing HDSs and aerodynamic means of debris removal can be estimated from analysing studies [10–18]. Thus, it is proposed in [10, 11] to use a permanent magnet harpoon system for SDOs, which increases the reliability of the harpoon devices of SD removal. Also, the onboard energy consumption is reduced compared to the transfer of an SDO to a lower orbit with the help of a motor CSC. This system is implemented by using an active-passive method of taking the SDOs out of an orbit when combining the benefits of active CSC with harpoons and passive PMDSs. However, the current state of this concept is at the level of theoretical substantiation and ground experiments. This is explained by the novelty of this concept, where preparation for space trials is ongoing.

Another example of the development of HDSs is the refinement of the concept of “an ion-beam shepherd (IBS)” by equipping the CSC with an aerodynamic compensator [12]. This technical solution enables to save the onboard energy required to compensate for the CSC impulse by means of an electro-jet engine during ion beam switching on. However, in [12] it is shown that the weight and complexity of the design of the aerodynamic compensator do not give obvious advantages for its current application.

Sailing [13–17] and transformed ADDSs [18] are similar in principle to the proposed system. These systems are passive means of clearing Earth’s space from SDOs, where the removal process itself is performed without managing the relative position of the SDOs against the ADDSs. However, considerable scientific interest in the development of sailboats and transformed ADDSs requires new engineering solutions to expand the boundaries of effective use of these facilities. In [13], it was proposed to have a sailing ADDS that can be deployed using a special inflatable mast. On 23 June 2017, a CubeSat 3U class spacecraft was launched and space testing of this system was performed in a 505 km sun-synchronous orbit. The tests confirmed that the height of the spacecraft after the sail deployment began to decrease significantly and the spacecraft reached dense atmospheric layers in 72 days. However, as noted earlier, the deorbiting was implemented using the passive method, without aligning the aerodynamic element perpendicular to the vector of the dynamic flow of the incoming atmosphere. According to the tests, [14] showed that if the orientation of the ADDS sails is perpendicular to the aerodynamic flow of the incoming atmosphere, it reduces the time of removing SDOs by about 20–40 %. However, to date, this issue has not been resolved, which is explained by the high cost of onboard energy to control the orientation of the system “Removable SD–ADDs”. AELDOS sailing systems [15] and those described in [16, 17]

as well as the transformed system [18] have the same disadvantages related to the orientation of the aerodynamic element. The absence of stabilization perpendicular to the dynamic flow of the incoming atmosphere in the systems listed above is also due to the complexity of developing the least energy-efficient control system of the relative position of the aerodynamic element.

Another example of the development of HDSs, including aerodynamic modules, is the active-passive system presented in [19, 20]. This system consists of two submodules: the engine system and the aerodynamic element. This HDS is proposed to be used to remove SDOs from low Earth orbits. The removal is carried out in two stages, where the first stage is the transfer of the SD into an elliptical orbit with perigee in the height range up to 800 km. At these altitudes, the force of aerodynamic drag has a significant effect on the SDO movement. After that, the aerodynamic element becomes opened and the SD is removed passively, followed by combustion in dense atmospheric layers. However, it should be noted that sufficient fuel reserves to carry it into the required orbit are not available on every spacecraft that is deorbited at the end of active life. Moreover, the issue of equipping the SC with additional engine installations is quite complicated, since it requires additional space on the SC itself and entails considerable weight. Thus, the proposed system is suitable for spacecraft only with certain mass-size characteristics that allow the installation of this system on board.

In turn, in [21] an aeromagnetic deorbiting system (AMDS) was developed to remove SDOs from LEOs. This system is the closest in technical nature to the proposed system and is called ACADS (Attitude Control and Aerodynamic Drag Sail) [21]. In the ACADS, orientation control is implemented by applying electromagnetic coils to stabilize the aerodynamic sail element perpendicular to the dynamic flow of the incoming atmosphere. However, the ACADS has the disadvantage that it also has to do with the significant onboard energy consumption which is required for electromagnets to function. Hence, there are difficulties in the use of the ACADS in long-term missions to remove SDOs from LEOs. In addition, the prerequisite for the normal functioning of the ACADS is to ensure the reliable full operation of the onboard SC power systems, which is also quite difficult over long periods of time. Thus, given these shortcomings, the ACADS has not been widely used.

Taking into account the aforementioned limitations, the task is to find the most energy-efficient control systems for the orientation of the aerodynamic element of the AMDS. One such solution is the use of permanent magnet devices, which is the focus of the following study.

3. The aim and objectives of the study

The aim of the study is to develop a design chart of an aeromagnetic deorbiting system in which control of the orientation of the aerodynamic element is implemented with the help of special devices with permanent magnets with minimal energy consumption.

To achieve this aim, the following tasks were set and done:

- to consider using permanent magnet controllers to stabilize aerodynamically unstable space objects;
- to carry out research on the feasibility of the method of applying the aeromagnetic system for deorbiting SDOs;

– to analyse the orbital motion of spacecraft with the AMDS and to determine the advantages in the removal time.

4. Analysis of the feasibility of using permanent magnet controllers for aerodynamically unstable space objects

The structural design of the AMDS HDS includes two main modules: the aerodynamic sailing element (ADSE) 7 and the biaxial orientation system with permanent magnets 2 (Fig. 1) [22]. This system is proposed for aerodynamically unstable SC with ADDSs (Fig. 1), which require additional stabilization of the aerodynamic elements with a maximum area perpendicular to the aerodynamic flow of the incoming atmosphere. The orientation of the spacecraft with the AMDS is performed in the orbital coordinate system (OCS).

The biaxial orientation system for permanent magnets consists of PMs 8, which are attached to the rotary actuators on micro stepper motors 9. In turn, the micro stepper motors 9 with the permanent magnets 8, orthogonal to one another, are mounted on the SC body mounts 10. The PMs are shielded with special screen capsules 3, which, if necessary, are opened and closed in a certain algorithm. Control of the opening and closing of the screen capsules is carried out on the electronic control node of the opening-closing (O-C CN) 4 with the help of special transfer mechanisms 5. In the closed state, the shutters of the screen capsules are placed into special niches 6, which are located in the SC body 1 (Fig. 1).

The AMDS operates according to a special algorithm. Thus, after the expiration of the active operation of the SC 1 and the deployment of the aerodynamic element 7, there is the orientation of the aerodynamic element of the AMDS in the OCS perpendicular to the vector of the dynamic flow of the atmosphere. The orientation is implemented by means of magnetic controls 2 with rotating permanent magnets (Fig. 1). The biaxial orientation is provided through the generation of discrete control moments, which are generated by the interaction of the permanent magnets 8 of the magnetic controls 2 with Earth's magnetic field (EMF). The opening and closing of the screen capsules 3 of the magnetic controls 2 provide the necessary algorithm for generating discrete control moments. The micro stepper motors 9 rotate the permanent magnets 8 180 degrees (Fig. 2) according to a certain algorithm and thus provide the required polarity of the dipole moments and hence the necessary positive or negative signs of the discrete control moments.

For screen capsules, a multilayer shielding material is proposed to consist of two layers of copper material, two layers of magnetic material, and an aluminium inner frame [23, 24]. According to the laboratory tests, this shielding material shields a permanent magnetic field with an induction of up

to 2 mT. Magnetic material AlNiCo5 was selected as a PM for control bodies; it has the most suitable magnetic and thermophysical characteristics for use in the conditions of LEOs [25].

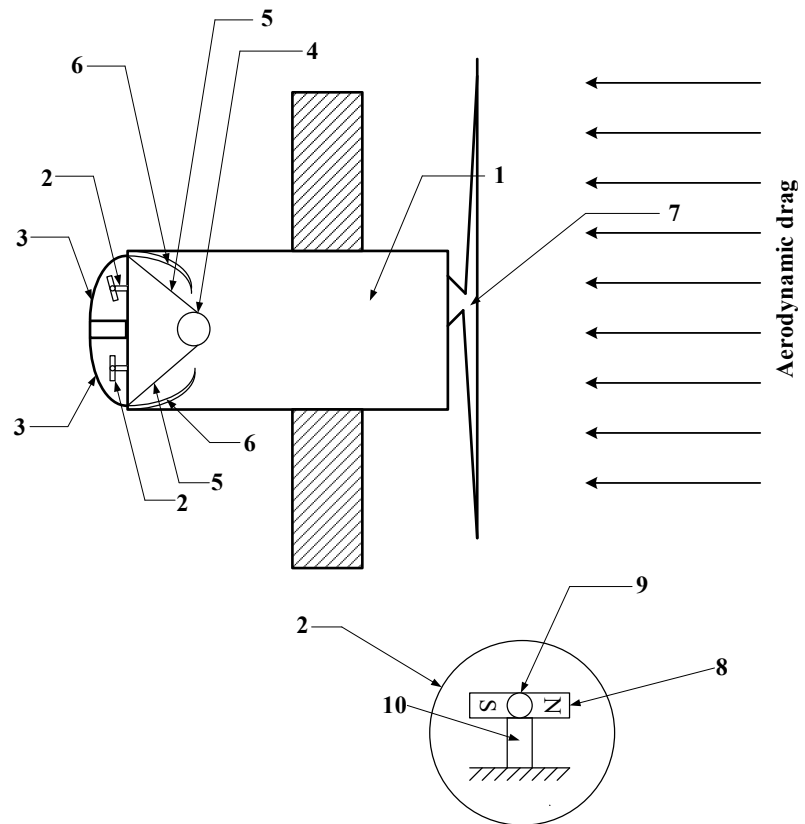


Fig. 1. The structural design of the AMDS HDS: 1 – the deorbited SC; 2 – the biaxial orientation system with permanent magnets; 3 – screen capsules; 4 – the electronic control node of the opening-closing (O-C CN); 5 – transmission mechanisms; 6 – niches for the screen capsules in the closed state; 7 – the ADSE; 8 – a permanent magnet; 9 – a micro stepper motor that rotates a permanent magnet; 10 – special attachments of permanent magnets to the body of the spacecraft

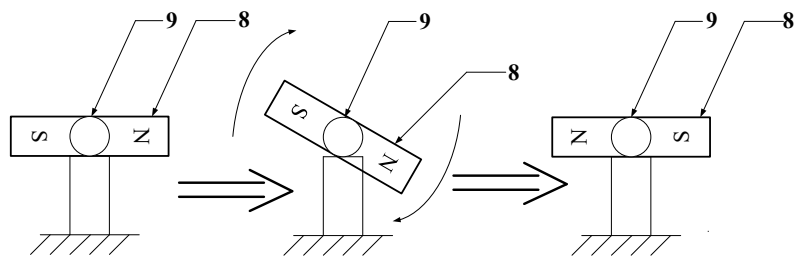


Fig. 2. Rotation of the permanent magnet 180° to provide the required sign of the discrete control moment: 8 – permanent magnet; 9 – a micro stepper motor that rotates the permanent magnet

5. Mathematical models to study orbital motion and to calculate the time of SC deorbiting with the help of the AMDS

Two systems of differential equations are proposed for the extensive study of the orbital motion and the calculations of the SC deorbiting time using the AMDS [26, 27]. The first system of differential equations is represented in

oscillating orbital elements, where derivatives are taken by the true anomaly ϑ :

$$\left. \begin{aligned} \frac{da}{d\vartheta} &= \frac{2pr_{sc}^2}{\mu(1-e^2)^2} \left(S \cdot e \sin \vartheta + T \cdot \frac{p}{r_{sc}} \right), \\ \frac{de}{d\vartheta} &= \frac{r_{sc}^2}{\mu} \left\{ S \cdot \sin \vartheta + T \cdot \cos \vartheta \left(1 + \frac{r_{sc}}{p} \right) + T \cdot e \frac{r_{sc}}{p} \right\}, \\ \frac{di}{d\vartheta} &= \frac{r_{sc}^3}{\mu p} \cos(\vartheta + \omega) \cdot W, \\ \frac{d\Omega}{d\vartheta} &= \frac{r_{sc}^3 \sin(\vartheta + \omega)}{\mu p \sin i} W, \\ \frac{d\omega}{d\vartheta} &= \frac{r_{sc}^2}{\mu e} \left\{ -\cos \vartheta S + \left(1 + \frac{r_{sc}}{p} \right) \sin \vartheta T \right\} - \\ &\quad - \cos i \frac{r_{sc}^3 \sin(\vartheta + \omega)}{\mu p \sin i} W, \\ \frac{dt}{d\vartheta} &= \frac{r_{sc}^2}{\sqrt{\mu p}} \left\{ 1 + \frac{r_{sc}^2}{\mu e} \left[\cos \vartheta S - \left(1 + \frac{r_{sc}}{p} \right) \sin \vartheta T \right] \right\}, \end{aligned} \right\} \quad (1)$$

where

- a is a large half-axis of the orbit;
- e is eccentricity of the orbit;
- Ω is the direct ascent of the ascending node;
- ω is the perigee argument;
- μ is the gravity constant, $\mu=3.986 \cdot 10^5 \text{ km}^3/\text{s}^2$;
- r_{sc} is the spacecraft vector radius, $r_{sc} = \frac{a(1-e^2)}{1+e \cos \vartheta}$;
- p is the focal parameter of the orbit, $p = a(1-e^2)$;
- i is obliqueness of the orbit;
- ϑ is a true anomaly;
- t is motion time in the orbit;
- $S, T,$ and W are projections of radial, transversal, and normal perturbing accelerations on the OCS axis.

In this case, the acceleration, gravitational, magnetic (interaction of the PMs with charged particles of ionospheric plasma and with the EMF) and aerodynamic perturbations are taken into account. However, it should be noted that the system of differential equations (1) is not suitable for describing the orbital motion of a spacecraft having an orbit with $e < 0.005$, since these values are too small and the solution degenerates. With this feature, a system of differential equations is proposed to calculate the diversion time from nearly circular low Earth orbits with $e < 0.005$ [27]:

$$\left. \begin{aligned} \frac{di}{dt} &= z \cos u \cdot W^*, \\ \frac{d\Omega}{dt} &= z \frac{\sin u}{\sin i} \cdot W^*, \\ \frac{du}{dt} &= \sqrt{\frac{\mu}{R_0^3}} \left(\frac{1}{z^2} - 1 \right) - z \frac{\sin u}{\sin i} \cdot \cos i \cdot W^* + \sqrt{\frac{\mu}{R_0^3}}, \\ \frac{d\gamma}{dt} &= 2 \cdot z \cdot s \cdot T^*, \\ \frac{db_1}{dt} &= \sqrt{\frac{\mu}{R_0^3}} b_2, \\ \frac{db_2}{dt} &= \sqrt{\frac{\mu}{R_0^3}} \frac{\gamma - b_1}{z^3} + S^*, \end{aligned} \right\} \quad (2)$$

where

- u is the latitude argument;
- R_0 is the radius of the undisturbed circular orbit;
- $b_1 = \frac{R}{R_0} - 1$ is the deviation of the current radius of the disturbed orbit R from the orbital radius;
- b_2 is the radial velocity in a disturbed orbit related to the velocity of motion in the undisturbed circular orbit;
- $z = 1 + b_1$;
- $\gamma = \frac{p}{R_0} - 1$ is a very low coefficient;
- $s = 1 + \gamma$;
- $S^* = \sqrt{\frac{R_0}{\mu}} \cdot S$;
- $T^* = \sqrt{\frac{R_0}{\mu \cdot s}} \cdot T$;
- $W^* = \sqrt{\frac{R_0}{\mu \cdot s}} \cdot W$.

In turn, the dynamic Euler equations are used to analyse motion around the centre of mass as follows:

$$\left. \begin{aligned} J_x \frac{d\omega_x}{dt} + \omega_y \omega_z (J_z - J_y) &= M_{x.ctrl.} + \sum M_{x.dist.}, \\ J_y \frac{d\omega_y}{dt} + \omega_x \omega_z (J_x - J_z) &= M_{y.ctrl.} + \sum M_{y.dist.}, \\ J_z \frac{d\omega_z}{dt} + \omega_y \omega_x (J_y - J_x) &= M_{z.ctrl.} + \sum M_{z.dist.}, \end{aligned} \right\} \quad (3)$$

where

- J_x, J_y, J_z are the main central moments of inertia of an SC with the AMDS;
- $\omega_x, \omega_y, \omega_z$ are the projections of the absolute angular velocity of the spacecraft on the axis of the fixed coordinate system (FCS);
- $M_{x.ctrl.}, M_{y.ctrl.}, M_{z.ctrl.}$ are the projections of the control moment on the FCS axis;
- $M_{x.dist.}, M_{y.dist.}, M_{z.dist.}$ are the projections of disturbance moments on the FCS axis.

Thus, the calculations take into account the aerodynamic and gravitational moments acting on the SC with the AMDS. To calculate the angles of yaw ψ , roll ϕ and pitch θ , the equations in the quaternionic form are used, which are given in [6].

6. Investigation of the AMDS efficiency when applying the discrete control of the relative position of the aerodynamic element

As mentioned above, PMs are used for the control system of the SC orientation with the AMDS. The moment M_{magn} that arises when the PMs interact with the external magnetic field, which is served by the EMF, is calculated by the following formula:

$$M_{magn.} = p_m \times V_{EMF}, \quad (4)$$

where p_m is the PM magnetic dipole moment; V_{EMF} is the vector of the EMF magnetic induction.

Given the need to generate discrete control points, it is proposed to apply a discrete method of controlling the magnetic actuators, which is given in [28]. Taking into account the implementation of the biaxial orientation by the yaw and the pitch, the projections of the control points on the FCS are recorded as follows:

$$\begin{aligned}
 M_{x.ctrl} &= p_{my} \cdot V_{z.EMF} - p_{mz} \cdot V_{y.EMF}, \\
 M_{y.ctrl} &= \text{sign}(\delta_y) \cdot p_{mz} \cdot V_{x.EMF}, \\
 M_{z.ctrl} &= \text{sign}(\delta_z) \cdot (-p_{my} \cdot V_{x.EMF}),
 \end{aligned}
 \tag{5}$$

where p_{my} and p_{mz} are the values of the magnetic dipole moments in the control channels by the pitch and the yaw; $V_{x.EMF}$, $V_{y.EMF}$, and $V_{z.EMF}$ are the projections of the magnetic induction vector of the EMF on the FCS axis; δ_y, δ_z are the function of the sign of the control moments provided by the PM rotary units.

According to expression (5), the first channel, with the roll control, is unmanaged. This is due to the fact that the rotation of the sail in the plane perpendicular to the vector of the dynamic flow of the incoming atmosphere does not practically affect the force of aerodynamic resistance (the force of the SD deceleration). Thus, for the orientation of the aerodynamic element of the SC with the AMDS, it is advisable to use a biaxial orientation in the yaw and the pitch. To calculate the opening frequency of the screen capsules and the PM rotation with the help of micro stepper motors, it is proposed to use the nonlinear control law and the pulse width modulator (PWM). In turn, the pulse width is calculated by the formula [29, 30]:

$$t_{amp} = \frac{M_{theor} \cdot T}{M_{ctrl}},
 \tag{6}$$

where M_{theor} is the theoretically calculated value of the control moment at the output of the regulator; M_{ctrl} is the value of the control point in the pitch and yaw channel; T is the sample period of the controller.

Thus, for the study of the efficiency of the AMDS method, a SC with the AMDS was selected with the characteristics given in Table 1:

Table 1

Characteristics of the SC with the AMDS

The mass of the spacecraft, m_{SC}	180 kg
J_x	17.995 kg·m ²
J_y	20.711 kg·m ²
J_z	15.269 kg·m ²
The area of the SC midsection, S_m	0.58 m ²
The area of the aerodynamic element of the AMDS, S_{AMDS}	5 m ²
The mass of the AMDS (with magnetic controls), m_{AMDS}	8 kg
The magnetic dipole moment of permanent magnets p_{my} and p_{mz}	15 A·m ²
Distance from the centre of mass to the centre of pressure r_b	0.12 m

Using mathematical and computer simulation for altitudes of 600 km and a period of 10,800 s, values were obtained to stabilise the spacecraft with the AMDS at the angles of the yaw and the pitch. In turn, the values of the discrete control points $M_{y.ctrl}$ and $M_{z.ctrl}$ as well as the required pulse frequency for their generation were also calculated. For the initial deviations, the angles of the yaw and the pitch were taken as $\psi=60^\circ, \theta=45^\circ$. The results of simulating the stabilization of the SC with the AMDS are presented in Fig. 3–8.

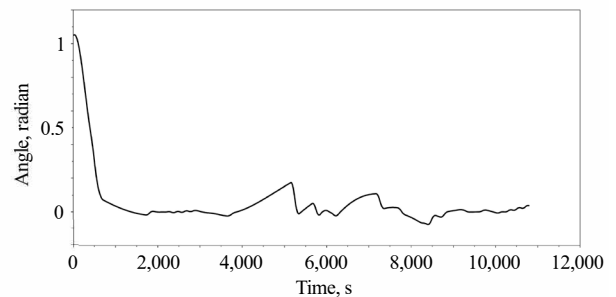


Fig. 3. Stabilization by the yaw

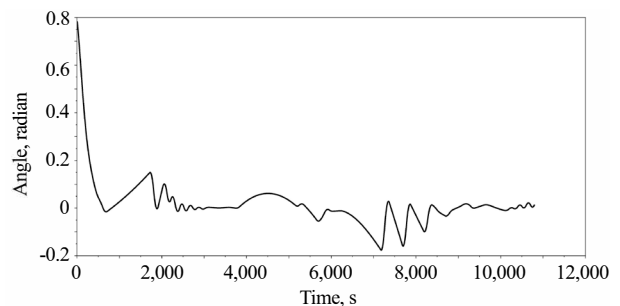


Fig. 4. Stabilization by the pitch

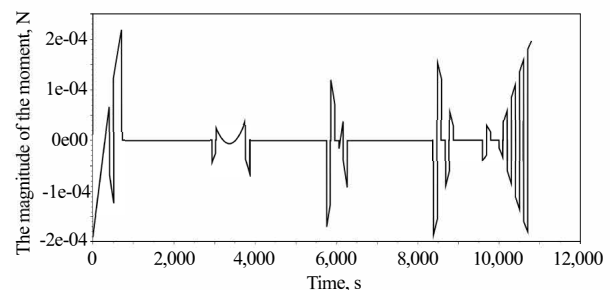


Fig. 5. The guiding moment to ensure stabilization by the yaw

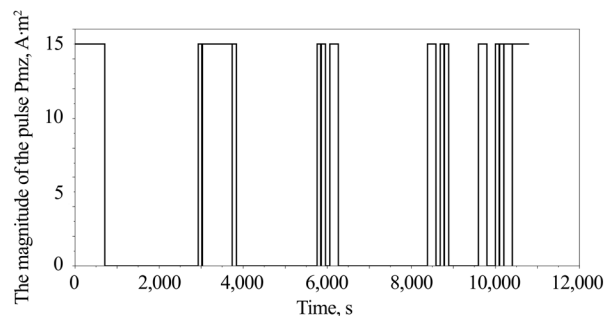


Fig. 6. The number of pulses to generate the control moment $M_{z.ctrl}$

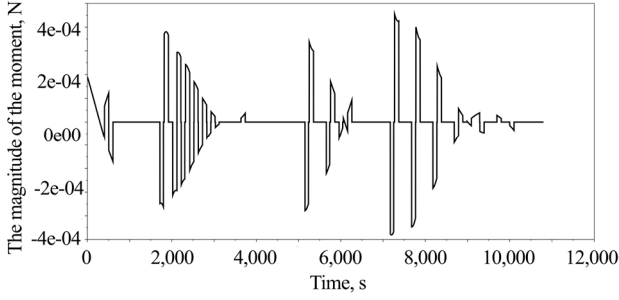


Fig. 7. The control moment to ensure stabilization by the pitch

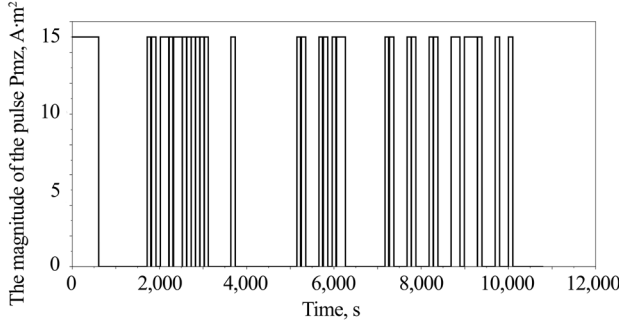


Fig. 8. The number of pulses to generate the control moment $M_{y,ctrl}$

It should be noted that in order to save the onboard energy, an impulse duration limit of at least 80 s was introduced, that is, short pulses requiring frequent opening and closing of the screen capsules were not generated. In turn, the modulus of absolute deviation of stabilization by the yaw and the pitch Δ did not exceed $0.2 \text{ rad} \approx 11.46^\circ$ (Fig. 2, 3). This is a good result for this task, since a completely accurate orientation of the aerodynamic element of the AMDS is not required. Thus, the cosine of maximum deviation is $\cos(11.46^\circ) \approx 0.98$, which satisfies the control accuracy in this problem. This is because the projection of the area of the aerodynamic element pr_SAMDS on the plane perpendicular to the aerodynamic flow of the incident atmosphere is 3.92 m^2 , which is only 2 % less than the total area SAMDS. The aerodynamic drag force F_{aero} is calculated by the following formula:

$$F_{aero.} = C_x \frac{\rho \cdot v^2}{2} S_{mid.}, \quad (7)$$

where C_x is the coefficient of aerodynamic resistance; ρ is the density of the atmosphere; v is the orbital velocity; S_{mid} is the area of the midsection (cross-sectional area of the spacecraft).

Thus, the aerodynamic drag force, which is directly proportional to the cross-sectional area of the spacecraft that is oriented to the dynamic flow of the incoming atmosphere with a maximum deviation of the aerodynamic element of the AMDS, is reduced by only 2 %.

Thus, if 4 micro stepper motors, class NEMO-17 having two windings, are used, the characteristics for the opening and closing of the screen capsules and the rotating PMs are the following:

- the rated current of the winding $I_r=1.8 \text{ A}$;
- the rated voltage of the winding $U_r=3.25 \text{ V}$;

- the maximum number of revolutions per minute $n_{max}=500 \text{ rpm}$;
- the step angle $k=1.8^\circ$.

Thus, the winding power consumed is $Pr=Ur Ir=5.85 \text{ W}$. The power of the whole motor per unit of time is $P_{r,m}=2Pr=11.7 \text{ W}$. According to the calculations (Fig. 4–7), 15 openings and closures of a screen capsule and 35 rotations of a PM are needed to generate the required discrete control moment $M_{y,ctrl}$, as well as 30 openings and closures and 25 rotations of the PM for $M_{z,ctrl}$. Considering the engine speed, at the rated operation, we assume that the PM rotation lasts 1 s and the opening of the screen capsule takes 2 s. It should be noted that the screen capsules are closed with the help of an automatic spring device, which returns the gear mechanism to its original position with practically no onboard energy consumption. This device is part of the transmission mechanism 5 of the screen capsule opening and closing control system (Fig. 2). Based on this, the total onboard energy consumption for the period of 10,800 s (approximately two turns at an altitude of 600 km) to open the screen capsules is $E_{O-C}=(15+30) \cdot 2 \cdot P_{r,m}=1,053 \text{ J}$, and for the PM rotation in both channels, it is $E_{PM}=(25+35) \cdot 1 \cdot P_{r,m}=702 \text{ J}$. Then the total onboard energy costs for controlling the AMDS orientation for two turns are as follows:

$$E_{AMDS}=E_{O-C}+E_{PM}=1,053+702=1,755 \text{ J} \approx 0.0004875 \text{ kW}\cdot\text{h}.$$

At the same time, when using electromagnets MT15-1 by ZARM Technik (China) having a maximum dipole moment of $15 \text{ A}\cdot\text{m}^2$ (as in the proposed PM), the onboard energy consumption will be much lower. Thus, at the supply voltage $U_s=14 \text{ V}$ and the rated power $P_r=1.11 \text{ W}$, the total cost of stabilization electricity for the same period of motion is $2,100 \text{ J}$. The onboard energy consumption by the electromagnets, despite their much lower power, is greater because the total continuous control period is ten times greater than when using stepper motors and PMs.

It should also be noted that as the minimum impulse length increases to 100 s, the number of pulses required decreases. With a minimum impulse length of 100 s, virtually maintaining a maximum deviation of no more than 11.46° , the total energy consumption can be reduced to $1,111.5 \text{ W}$.

Thus, with the use of the discrete control law and PMs, the total energy costs can be reduced by 30–40 %, which is significant for long-term missions of SDO removal.

7. Calculation of the time of removing spacecraft using AMDSs from orbits of various dislocations

It is proposed to study the orbital motion of spacecraft with different AMDSs in order to evaluate the advantages in the time of removal by the AMDS compared to the ADDS (without stabilization to the vector of the flowing atmosphere). Thus, the study was conducted on nearly-circular LEOs and slightly-elliptic LEOs, which are almost similar to circular EOs but have a significant difference in altitudes in the apogee and the perigee (more than 100 km). In turn, a system of differential equations (2) is used to calculate the time of removal from the nearly-circular orbits, and a mathematical model (1) is used for the slightly-elliptic orbits. The results of calculating the allotment time for the proposed orbits of different inclinations are given in Table 2.

Table 2
The results of calculating the time of deorbiting spent spacecraft by using the AMDS

Nearly-circular LOEs with $e=0.00001$							
Orbit altitude, km	Tilt, deg.	SC weight, kg	AMDS weight, kg	Midsection area		Deorbiting time without the AMDS stabilization	Deorbiting time with the AMDS stabilization
				AMDS, m ²	SC, m ²		
600	90	180	8	5	0.58	4.15 years	3.12 years
700	80	180	8	5	0.58	17.37 years	13.44 years
750	60	180	8	5	0.58	32.76 years	26.5 years
Slightly-elliptic LOEs with $e=0.01$							
Height in the perigee	Height in the apogee	Tilt, deg.	Weight of the SC with the AMDS, kg	Midsection area		Deorbiting time without orientation of the aerod. elm.	Deorbiting time with orientation of the aerod. elm.
				AMDS	SC		
600	740.82	80	188	5	0.58	5.49 years	4.25 years
700	842.85	20	188	5	0.58	22.44 years	18.2 years

Table 2 shows that the advantages of using the AMDS have been determined according to the performed tests of the orbital motion of the spacecraft with the AMDS and the calculations of the time it takes to deorbit the spacecraft using the AMDS in orbits up to an altitude of 180 km. Thus, the orientation of the aerodynamic element of the AMDS perpendicular to the vector of the dynamic flowing of the atmosphere provides a 23–24 % gain in the withdrawal time and extends the boundaries of the effective application of this deorbiting system. However, it should be noted that the method of orienting the aerodynamic element in comparison with the non-orientated deorbiting gives time benefit only for aerodynamic and transformed sailing systems. This is because the area of the midsection in such systems is much greater than the fourth part of the area of the full surface

$S_{f.s.}$ of the aerodynamic element, that is, $S_{mid.} \gg \frac{1}{4} S_{f.s.}$.

8. Discussion of the results of studying the possibility of using ADDSs to deorbit SDOs from LEOs

The conducted tests have shown the possibility of using magnetic controls with permanent magnets for aerodynamically unstable space structures (a spacecraft+an aerodynamic deorbiting system). The design chart (Fig. 1) suggests the possible attachment of magnetic controls with permanent magnets, and Fig. 2 gives a view of rotating magnets. The use of a discrete nonlinear controller in Section 6 has proved the possibility of stabilizing the aerodynamically unstable coupling of the spacecraft with the AMDS in the orbital coordinate system with a maximum area perpendicular to the dynamic flow of the incoming atmosphere. Such orientation makes it possible to increase the force of aerodynamic resistance (7) and hence to reduce the deorbiting time of the exhausted spacecraft. The quality of the

biaxial stabilization of the spacecraft with the AMDS (Fig. 3, 4) when using a nonlinear discrete controller (5), (6) (Fig. 5–8) has confirmed the effectiveness of the proposed magnetic controls. The calculations have shown that the use of low-cost stepping motors allows reducing the onboard energy consumption for orientation compared to the prototype system [21].

Using the mathematical models of the orbital motion of the spacecraft (1), (2), the time of deorbiting the spent spacecraft with the help of the AMDS was calculated and the limits of the effective application of the AMDS were revealed. The advantages of using AMDSs in comparison with aerodynamically unstable sailing ADDSs were also identified.

However, as stated in [19], the AMDS has limitations on the choice of magnetic material for permanent magnets that would be suitable for operating conditions within a LEO. Also, there may be difficulties with the temperature operation of stepper motors in Earth’s outer space environment. However, in the case of actively developed thermoregulating coatings, these problems can be eliminated.

It should also be noted that mathematical and computer simulations do not provide complete information regarding the effectiveness of AMDSs. Therefore, a prerequisite is to conduct summer tests in outer space.

Therefore, further studies should be of experimental design in order to find the necessary design parameters of the AMDS for a particular spacecraft.

9. Conclusion

1. The possibility of using permanent magnet controls to stabilize the relative position of a spacecraft with the aerodynamic element has been analysed. A constructive chart of the aeromagnetic system to deorbit SC from LEOs has been developed. The peculiarity of the AMDS design is that the controls of the relative position of the aerodynamic element are rotary permanent magnets that are shielded by means of special screen capsules with shutters.

2. The efficiency of the method of applying the aeromagnetic system to deorbit the SD was analysed when using a nonlinear discrete controller.

3. The benefits of using the AMDS were identified in comparison with passive ADDSs. Indeed, the mathematical and computer simulations in the SciLab application package have shown that with the use of the AMDS the time of deorbiting a spent spacecraft is reduced by about a quarter, which is quite significant in long-term missions.

References

1. Orbital Debris Quarterly News (2019). National Aeronautics and Space Administration, 23 (1-2). Available at: <https://orbitaldebris.jsc.nasa.gov/quarterly-news/pdfs/odqnv23i1.pdf>
2. Alpatov, A. P., Goldstein, Yu. M. (2017). Ballistic Analysis of Orbits Distribution of Spacecraft for Different Functional Missions. Technical Mechanics, 2, 33–40.

3. Alpatov, A. P., Holdshstein, Yu. M. (2019). On the choice of the ballistic parameters of an on-orbit service spacecraft. *Technical Mechanics*, 1, 25–37. Available at: <http://www.journal-itm.dp.ua/docs//P-03-01-2019.pdf>
4. Paliy, A. S. (2012). Metody i sredstva uvoda kosmicheskikh apparatov s rabochih orbit (sostoyanie problemy). *Technical Mechanics*, 1, 94–102.
5. Alpatov, A. P. (2012). *Tehnogennoe zasorenie okolozemnogo kosmicheskogo prostranstva*. Dnepropetrovsk: Porogi, 378.
6. Alpatov, A. P., Khoroshylov, S. V., Maslova, A. I. (2019). Contactless de-orbiting of space debris by the ion beam. *Dynamics and control*. Kyiv: Akadempriodyka, 170. doi: <https://doi.org/10.15407/akadempriodyka.383.170>
7. Pikalov, R. S., Yudinsev, V. V. (2018). Obzor i vybor sredstv uvoda krupnogabaritnogo kosmicheskogo musora. *Trudy MAI*, 100. Available at: http://trudymai.ru/upload/iblock/239/Pikalov_YUdintsev_rus.pdf?lang=ru&issue=100
8. Dron, N. M., Horolsky, P. G., Dubovik, L. G. (2014). Ways of reduction of technogenic pollution of the near-earth space. *Naukovyi Visnyk Natsionalnoho hirnychoho universytetu*, 3, 125–130.
9. Lapkhanov E. O. (2019). Features of the development of means for spacecraft removal from near-earth operational orbits. *Technical Mechanics*, 2, 16–29.
10. Shuvalov, V. O., Paliy, O. S., Lapkhanov, E. O. (2018). Zaiavka na Pat. No. a201801742 UA. Sposib ochyshchennia navkolozemnoho prostoru vid ob'ektiv kosmichnoho smittia shliakhom vidvedennia yikh z orbity za dopomohoiu vlasnoho mahnitnoho polia. MPK B 64 G 1/62. No. a201801742; declared: 21.02.2018.
11. Shuvalov, V. A., Gorev, N. B., Tokmak, N. A., Pis'mennyi, N. I., Kochubei, G. S. (2018). Control of the drag on a spacecraft in the earth's ionosphere using the spacecraft's magnetic field. *Acta Astronautica*, 151, 717–725. doi: <https://doi.org/10.1016/j.actaastro.2018.06.038>
12. Svorobin, D. S., Fokov, A. A., Khoroshylov, S. V. (2018). Feasibility analysis of aerodynamic compensator application in noncontact space debris removal. *Aerospace technic and technology*, 6, 4–11. doi: <https://doi.org/10.32620/akt.2018.6.01>
13. Underwood, C., Viquerat, A., Schenk, M., Taylor, B., Massimiani, C., Duke, R. et. al. (2019). InflateSail de-orbit flight demonstration results and follow-on drag-sail applications. *Acta Astronautica*, 162, 344–358. doi: <https://doi.org/10.1016/j.actaastro.2019.05.054>
14. Trofimov, S. P. (2015). Deorbiting of low-earth orbit spacecraft using a sail for solar radiation pressure force augmentation. Preprint IPM im. M. V. Keldysha, 32. Available at: https://keldysh.ru/papers/2015/prep2015_32.pdf
15. Harkness, P., McRobb, M., Lützkendorf, P., Milligan, R., Feeney, A., Clark, C. (2014). Development status of AEOLDOS – A deorbit module for small satellites. *Advances in Space Research*, 54 (1), 82–91. doi: <https://doi.org/10.1016/j.asr.2014.03.022>
16. Anderson, J. L. NASA's Nanosail-D 'Sails' Home – Mission Complete. NASA. Available at: https://www.nasa.gov/mission_pages/smallsats/11-148.html
17. Bernardi, F., Vignali, G. SSCD: Sailing System for Cubesat Deorbiting. Available at: http://www.unisec-global.org/ddc/pdf/1st/01_FedericoSailing_abst.pdf
18. Paliy, O. S. (2017). Classification of aerodynamic systems for low Earth orbit space hardware deorbiting. *Technical Mechanics*, 4, 49–54.
19. Dron', M., Golubek, A., Dubovik, L., Dreus, A., Heti, K. (2019). Analysis of ballistic aspects in the combined method for removing space objects from the near-Earth orbits. *Eastern-European Journal of Enterprise Technologies*, 2 (5 (98)), 49–54. doi: <https://doi.org/10.15587/1729-4061.2019.161778>
20. Dron, M., Dreus, A., Golubek, A., Abramovsky, Y. (2018). Investigation of aerodynamics heating of space debris object at reentry to earth atmosphere. 16th IAA Symposium on space debris, Bremen. IAC-18,A6,IP,39,×43826, 7.
21. Pfisterer, M., Schillo, K., Valle, C., Lin, K.-C., Ham, C. The Development of a Propellantless Space Debris Mitigation Drag Sail for LEO Satellites. Available at: <http://www.iiis.org/Chan.pdf>
22. Khoroshylov, S. V., Paliy, O. S., Lapkhanov, E. O. (2019). Zaiavka na Pat. na vynakhid No. a201907950 UA. Aeromahnitna systema vidvedennia ob'ektiv kosmichnoho smittia z nyzkykh navkolozemnykh orbit z mahnitnymi orhanamy keruvannia. MPK B 64 G 1/62. No. a201907950, declared: 11.07.2019.
23. Dmitrenko, V. V., Nyunt, P. W., Vlasik, K. F., Grachev, V. M., Grabchikov, S. S., Muravyev-Smirnov, S. S. et. al. (2015). Electromagnetic shields based on multilayer film structures. *Bulletin of the Lebedev Physics Institute*, 42 (2), 43–47. doi: <https://doi.org/10.3103/s1068335615020037>
24. Safonov, A. L., Safonov, L. I. (2015). Elektricheskie pryamougol'nye soediniteli. Mnogosloynnye metallizirovannye ekrany zashchity ot EMP i sposoby ih polucheniya. *Technologies in Electronic Industry*, 1, 64–69.
25. Coey, J. (2010). *Magnetism and magnetic materials*. Cambridge University Press. doi: <https://doi.org/10.1017/CBO9780511845000>
26. Fortescue, P., Swinerd, G., Stark, J. (Eds.) (2011). *Spacecraft Systems Engineering*. John Wiley & Sons Ltd. doi: <https://doi.org/10.1002/9781119971009>
27. Maslova, A. I., Pirozhenko, A. V. (2016). Orbit changes under the small constant deceleration. *Space Science and Technology*, 22 (6), 20–25. doi: <https://doi.org/10.15407/knit2016.06.020>
28. Alpatov, A. P. et. al. (1978). *Dinamika kosmicheskikh apparatov s magnitnymi sistemami upravleniya*. Moscow: Mashinostroenie, 200.
29. Khoroshylov, S. V. (2018). Relative Motion Control System of Spacecraft for Contactless Space Debris Removal. *Nauka Ta Innovacii*, 14 (4), 5–17. doi: <https://doi.org/10.15407/scin14.04.005>
30. Alpatov, A., Khoroshylov, S., Bombardelli, C. (2018). Relative control of an ion beam shepherd satellite using the impulse compensation thruster. *Acta Astronautica*, 151, 543–554. doi: <https://doi.org/10.1016/j.actaastro.2018.06.056>